On Horizontal Beams and Sound Radiation due to a Moving Load

[1]Nitin Agarwala, [2]E M Somashekharan Nair

[1]Hull Inspection and Trials Unit, Vishakhapatnam - 530 014, India
[2]Mechanical Engineering Department, SCMS School of Engineering and Technology, Palissery, Karukutty, Kochi, India

nitindu@yahoo.com

Abstract: Effect of loss factor, rotatory inertia and shear effect on sound radiation by horizontal beams subject to moving loads at subsonic speeds is analysed. Although the contribution of these factors may yield results only a few percentages more accurate and their effect is quite profound when dynamic response analysis is undertaken, it may be an overestimate for slender bodies. The problem is formulated for *Timoshenko beam*, *Rayleigh beam*, *Shear beam* and *Bernoulli-Euler beam* with complex shear and elastic modulus. Taking Fourier transform of the governing equation the non-dimensional sound radiation is obtained and compared to analyse the contributions of loss factor, rotatory inertia and shear effect on sound radiation. The results show that a Timoshenko beam gives the least sound radiation power when compared with other beam types. The magnitude of sound radiation limited to a maximum of 4-5 % increases as one moves from the Shear beam to the Rayleigh beam to the Bernoulli beam. The effect of structural damping exhibits a relation inversely proportional to the vibration levels. The shift of curves due to damping variation is however found to be proportional to the change in the loss factor.

Keywords: Moving Load; Bernoulli-Euler Beam; Rayleigh Beam; Shear Beam; Timoshenko Beam; Loss Factor; Heavy fluid-loading; Sound radiation.

Introduction

A ship at sea or an aircraft in flight vibrate due to surface forces applied by the relative motion of the fluid they are traveling in. Larger the magnitude of the moving load, higher the vibration. High vibration levels generate noise or cause material failure, thus degrading the structure's performance. In case of a floating airport, a bridge, guideway, overhead crane, cableways, rails or roadways the structure is static while being subject to moving loads; unlike the case of a ship or an aircraft wherein the structure is moving and the surface force is at rest. May it be a moving structure in static fluid; a moving force over a static structure or both the force and the structure moving; the resultant effect is vibrations, which cause degradation of the structure.

Moving loads on structures have been analyzed ever since the first railway bridge was built in the early19th century. Over the years, such studies have been the subject of various investigations, and hence an extensive bibliography is available. A comprehensive treatment of the subject of vibrations of structures due to moving loads which contains a large number of related cases is given by Fryba (1999). Theoretically, the problem of moving load was first tackled for a case in which the beam mass was considered small against the mass of a single, constant load. The original approximate solution is due to R. Willis et. al. (1851) one of the early experimenters in the field. Since then these problems has become more dynamic in character mainly due to the increased vehicle speed and structural flexibility. What remains however common in these is the idealization of the structure as a string, a beam or a plate. This is done not only due to the frequent occurrences of these structures in several engineering disciplines, but also to simplify the mathematical structure of the governing equations compared with a full three-dimensional equation. Ever since the Classical Beam Theory was used to construct the Eiffel Tower and the Ferris wheel in the late 19th century, the Bernoulli-Euler beam theory has become a cornerstone of engineering for use in the analysis of structures. By neglecting the terms of shear effect and rotatory inertia, one arrives at the Bernoulli-Euler Beam from the Timoshenko beam. The contribution of these terms changes the accuracy of the results by a very small percentage; however, for dynamic analysis these components cannot be neglected.

The phenomenon of acoustics of vibrating structures caught the attention of Lord Rayleigh (1896). Techniques for dealing with fully coupled motions of elastic plates and shells immersed in air or water were simply not available in Rayleigh's time, but have become available in the past three decades or so. A standard reference on the analytical modeling is the book of Junger and Feit (1986). Early investigations of sound radiation from a force excited, elastic, fluid-loaded plate by Gutin (1965), Maidanik and Kerwin (1967) and Feit (1967) were primarily for the far field pressure and power radiated into the acoustic medium. Nayak (1970), using the Fourier integral representation of the solution evaluated the velocity response numerically to determine the drive line admittance for a line-driven plate. Crighton in a series of papers Crighton (1972, 1977, 1979 and 1983) analyzed both the near-and far field responses of locally excited plates. Crighton's results although probably the most complete to date in this field, are somewhat difficult to visualize due to the complexity of the problem and that they have not been displayed in a graphical form.

The sound radiation from a moving force excited, elastic structure is a relatively newer area of interest. Keltie and Peng (1989) investigated the sound radiation from a fluid-loaded Timoshenko beam subject to a moving harmonic line force. Results show that for beams under light fluid loading, the coincidence sound radiation peak for a stationary force gets split into two coincidence peaks due to the effects of the Doppler shift, while for beams under heavy fluid loading there are no pronounced sound radiation peaks. Following the study of Keltie, Cheng and Chui (1999) formulated the vibration response of periodically simply supported beam on the whole structure in wave-number domain through Fourier transform. This problem was an advance on traditional substructure methods. For an air-loaded beam subjected to a stationary line force, they showed that the radiated sound power exhibited peaks at certain wave-number ratios. The wave-number ratios at which radiation peaks occur nearly coincide with the lower bounding wave-number ratios of the odd number of propagation zones. However, Cheng's formulation did not include the presence of numerous wave-number components induced from the elastic supports and is subject to the restriction that the external force is located on one of the elastic supports. Cheng et al. (2000, 2001) introduced a "wave-number harmonic series" to discuss the vibro-acoustic response of a fluid-loaded beam on periodic elastic supports subjected to a moving load. Results show that the response of a beam on an elastic foundation can be approximated using a periodically, elastically supported beam when the support spacing is small compared with the flexural wavelength. For such beams when the force is stationary a single radiation peak occurs which splits into two peaks due to Doppler shift when the force becomes traveling.

The above mentioned studies of elastic beams excited by a moving force, have considered a Timoshenko beam with complex shear modulus and elastic modulus to cater for structural damping and dynamic response. However for long slender beams such as a floating airport, the Timoshenko beam may be an overkill. Similarly, assuming the presence of a loss factor, introduces a natural structural damping which needs to be ignored as there is no resonance mechanism for these floating structures. It is hence considered essential that the effect of the shear deformation and rotatory inertia on sound radiation from beams be studied to understand the best model for analysis. One needs to understand the effect of loss factor on sound radiation for these structures before disregarding their contribution. It is in this regard that the present study has been undertaken which provides a simple yet effective methodology in calculating the component of acoustic signature generated due to the relative motion (modeled as a moving load) of the ship (modeled as a beam) and the water when the ship is underway.

In this paper, damping characterized by the loss factor, often denoted by η, has been considered using a "constant loss factor" model. Including complex shear modulus and Elastic modulus (hence the loss factor); the problem has been formulated for the four beam types following the approach described by Keltie. Using Fourier transformation the total sound power is calculated and results presented at a range of frequencies both below and above coincidence for heavy fluid-loaded elastic beams. The acoustic power due to loss factor variation is additionally studied for a heavy fluid-loaded Timoshenko beam.

Formulation

The motion of an infinite beam excited by a force of length 2L moving at a subsonic speed V is formulated. The problem is considered in two-dimensional Cartesian co-ordinate system with x-axis being in the horizontal direction and y-axis in the vertically upward positive direction, as seen in Figure 1. The beam occupies the plane $y = 0$. The space $y>0$ is filled with an acoustic medium (water, air etc). The moving force may be assumed to be a uniform distributed line force given by $f(x,t) = \frac{f_0}{2L}[H(x - Vt + L) - H(x - Vt - L)]e^{j\omega t}$ or a point force given by $f(x,t) = f_0 e^{j\omega t}\delta(x - Vt)$

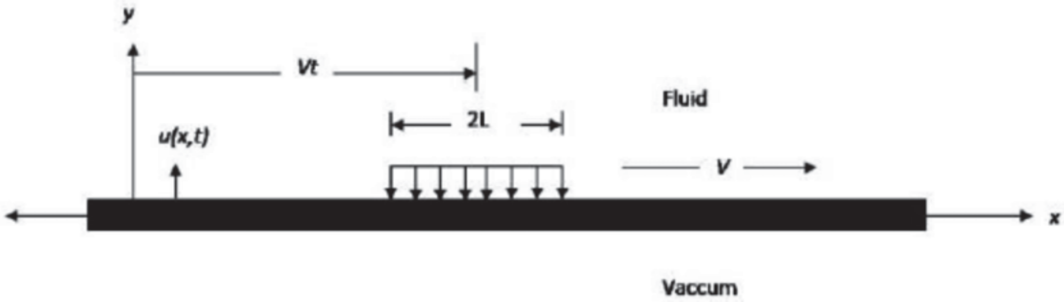

Figure 1: Schematic representation of the problem geometry

The vibration equation for the elastic beam, including rotational inertia and transverse shear effects, is given by Junger and Feit (1986) as

$$\bar{E}I\frac{\partial^4 u(x,t)}{\partial x^4}+\rho_v h\frac{\partial^2 u(x,t)}{\partial t^2}-\rho_v I\Big(1+\frac{\bar{E}\rho_v}{\kappa^2\bar{G}}\Big)\frac{\partial^4 u(x,t)}{\partial x^2\partial t^2}+\rho_v I\frac{\rho_v}{\kappa^2\bar{G}}\frac{\partial^4 u(x,t)}{\partial t^4}$$
$$=\Big(1-\frac{\bar{E}I}{\kappa^2\bar{G}h}\frac{\partial^2}{\partial x^2}+\frac{\rho_v h^2}{12\kappa^2\bar{G}}\frac{\partial^2}{\partial t^2}\Big)[f(x,t)-p(x,y=0,t)] \tag{1a}$$

From this equation follow three special cases:

(a) *Rayleigh beam*: If the effect of rotary inertia is considered and the effect of shear is neglected, the so called Rayleigh beam model results and equation (1a) reduces to

$$\bar{E}I\frac{\partial^4 u(x,t)}{\partial x^4}+\rho_v h\frac{\partial^2 u(x,t)}{\partial t^2}-\rho_v I\frac{\partial^4 u(x,t)}{\partial x^2\partial t^2}=[f(x,t)-p(x,y=0,t)] \tag{1b}$$

(b) *Shear Beam*: If the effect of rotatory inertia is neglected and effect of shear on the dynamic deflection of beam is considered, equation (1a) reduces to

$$\bar{E}I\frac{\partial^4 u(x,t)}{\partial x^4}+\rho_v h\frac{\partial^2 u(x,t)}{\partial t^2}-\frac{\bar{E}I\rho_v}{\kappa^2\bar{G}}\frac{\partial^4 u(x,t)}{\partial x^2\partial t^2}=(1-\frac{\bar{E}I}{\kappa^2\bar{G}h}\frac{\partial^2}{\partial x^2})[f(x,t)-p(x,y=0,t)] \tag{1c}$$

(c) *Bernoulli-Euler beam*: If we neglect the effect of both shear and rotatory inertia we obtain the classical Bernoulli-Euler beam model.

$$\bar{E}I\frac{\partial^4 u(x,t)}{\partial x^4}+\rho_v h\frac{\partial^2 u(x,t)}{\partial t^2}=[f(x,t)-p(x,y=0,t)] \tag{1d}$$

The pressure distribution induced by the vibrating beam in the acoustic medium is denoted by $p(x,y,t)$ and satisfies the wave equation in two-dimensional space, give by

$$(\frac{\partial^2}{\partial x^2}+\frac{\partial^2}{\partial y^2}-\frac{1}{C_0^2}\frac{\partial^2}{\partial t^2})p(x,y,t)=0 \tag{2}$$

The boundary condition at $y=0$ is given by

$$\rho_0\frac{\partial^2 u}{\partial t^2}=-\frac{\partial p}{\partial y}\Big|_{y=0} \tag{3}$$

By applying the spatial Fourier transformation $FT()=\int_{-\infty}^{\infty}()e^{i\xi x}dx$, with ξ as the wave number variable, the force function for a harmonic line force in wave number domain may be written as

$$\tilde{f}(\xi,t) = f_0 \frac{sin(\xi L)}{\xi L} e^{j(\omega+\xi V)t} = F(\xi) e^{j(\omega+\xi V)t} \tag{4a)(i}$$

and for a point force as

$$\tilde{f}(\xi,t) = f_0 e^{j(\omega+\xi V)t} = F(\xi) e^{j(\omega+\xi V)t} \tag{4a)(ii}$$

the transformed displacement as

$$\tilde{U}(\xi,t) = U(\xi) e^{j(\omega+\xi V)t} \tag{4b}$$

and the transformed pressure as

$$\tilde{P}(\xi,y,t) = P(\xi,y) e^{j(\omega+\xi V)t} \tag{4c}$$

Upon substitution of equation (4a), (4b) and (4c) in the relevant beam equation and the acoustic equation, we get

$$U(\xi) = \frac{Z_F F(\xi)}{Z_m + Z_F Z_a} \tag{5}$$

and

$$P(\xi, y=0) = \frac{j\rho_0(\omega+\xi V)^2}{K_y} U(\xi) \tag{6}$$

where the acoustic impedance operator (Z_a) for the *Timoshenko beam*, *Rayleigh beam*, *Shear beam* and *Bernoulli-Euler beam* is given by

$$Z_a = \frac{j\rho_0(\omega+\xi V)^2}{K_y} \tag{7}$$

the beam impedance operator (Z_m) as

$$Z_m = \bar{E}I\xi^4 - \rho_v h(\omega+\xi V)^2 - \xi^2 \rho_v I\left(1+\frac{\bar{E}\rho_v}{\kappa^2\bar{G}}\right)(\omega+\xi V)^2 + \rho_v I\frac{\rho_v}{\kappa^2\bar{G}}(\omega+\xi V)^2 \quad \text{Timoshenko beam} \tag{8a}$$

$$Z_m = \bar{E}I\xi^4 - \rho_v h(\omega+\xi V)^2 - \xi^2 \rho_v I(\omega+\xi V)^2 \quad \text{Rayleigh beam} \tag{8b}$$

$$Z_m = \bar{E}I\xi^4 - \rho_v h(\omega+\xi V)^2 - \xi^2 \frac{\bar{E}I\rho_v}{\kappa^2\bar{G}}(\omega+\xi V)^2 \quad \text{Shear beam} \tag{8c}$$

$$Z_m = \bar{E}I\xi^4 - \rho_v h(\omega+\xi V)^2 \quad \text{Bernoulli-Euler beam} \tag{8d}$$

the Z_F by

$$Z_F = 1 + \frac{\bar{E}I}{\kappa^2\bar{G}h}\xi^2 - \frac{\rho_v h^2}{12\kappa^2\bar{G}}(\omega+\xi V)^2 \quad \text{Timoshenko beam} \tag{9a}$$

$$Z_F = 1 \quad \text{Rayleigh beam} \tag{9b}$$

$$Z_F = 1 + \frac{\bar{E}I}{\kappa^2\bar{G}h}\xi^2 \quad \text{Shear beam} \tag{9c}$$

$$Z_F = 1 \quad \text{Bernoulli-Euler beam} \tag{9d}$$

and K_y is given by

$$K_y = \begin{cases} -j\sqrt{\xi^2 - (K_0 + M\xi)^2} & for \quad \xi^2 > (K_0 + M\xi)^2 \\ \sqrt{(K_0 + M\xi)^2 - \xi^2} & for \quad \xi^2 < (K_0 + M\xi)^2 \end{cases} \tag{10}$$

We shall now discuss the methodology of finding the total acoustic power.

Total Acoustic Power

The time averaged sound intensity is given by Morse and Ingrad (1986) as

$$\bar{I} = \frac{1}{T}\int_0^T \overline{PV}dt \quad or \quad \bar{I} = \frac{1}{2}Re[P\dot{U}^*]$$

In order to find the total acoustic power (Π), the surface acoustic intensity distribution needs to be integrated over the infinite length of the beam as

$$\Pi = \int_{-\infty}^{\infty} \frac{1}{2}Re[P(x, y=0,t)\dot{U}^*(x,t)]dx$$

Upon substituting the sound pressure (6) and calculating the surface velocity using (5), the sound power radiated per unit width of the beam can be simplified as

$$\Pi = \frac{\rho_0}{4\pi}Re\Big[\int_{-\infty}^{\infty} \frac{(\omega+\xi V)^3}{K_y} |U(\xi)|^2 \, d\xi\Big] \tag{11}$$

Limiting the study to subsonic motion of the moving load, the limits within which K_y is real is given by

$$\xi_1 = \frac{-K_0}{1+M} \le \xi \le \xi_2 = \frac{K_0}{1-M}$$

This allows us to rewrite the expression for the sound power as

$$\Pi = \frac{\rho_0}{4\pi}Re\Big[\int_{\xi_1}^{\xi_2} \frac{(\omega+\xi V)^3}{K_y} |U(\xi)|^2 \, d\xi\Big] \tag{12}$$

This completes the formulation of an expression for the total acoustic power for varying beam types subjected to a moving load.

Non-Dimensionalization

In order to present the numerical results, the concept of non-dimensional parameters defined in Keltie and Peng (1989) is used. Hence the dimensionless radiated sound power per unit width for a uniform distributed line force is given as

$$W = \int_{\zeta_1}^{\zeta_2} \alpha^3\beta \Big| Z_F \frac{sin(\zeta K_0 L)}{\zeta K_0 L} \Big|^2 |D|^{-2} \tag{13}$$

where

$$\zeta_1 = \frac{-1}{1+M} \le \zeta \le \zeta_2 = \frac{1}{1-M}$$

$$\alpha = 1 + M\zeta \;\$\$\; \beta = \sqrt{\alpha^2 - \zeta^2}$$

$$D = \beta(D_1 - D_2 + D_3) + jD_4$$

The expression for D_1, D_2, D_3, D_4 and Z_F vary based on the type of the beam as under

(a) *Timoshenko beam*:

$$Z_F = 1 + \frac{2(1+\nu)\gamma^4}{\kappa^2}\Big(\frac{C_0}{C_L}\Big)^2\Big[\zeta^2 - \frac{1}{1+\eta j}\Big(\frac{C_0}{C_L}\Big)^2\alpha^2\Big]$$

$$D_1 = \gamma^4\zeta^4(1+\eta j)$$

$$D_2 = \alpha^2\Big[1 + [1 + \frac{2(1+\nu)}{\kappa^2}]\gamma^4\zeta^2\Big(\frac{C_0}{C_L}\Big)^2\Big]$$

$$D_3 = \frac{2(1+\nu)}{\kappa^2(1+\eta j)}\alpha^4\gamma^4\Big(\frac{C_0}{C_L}\Big)^4$$

$$D_4 = Z_F \frac{\alpha_0 \alpha^2}{\gamma^2}$$

(b) *Rayleigh beam*:

$$Z_F = 1$$
$$D_1 = \gamma^4 \zeta^4 (1 + \eta j)$$
$$D_2 = \alpha^2 \left[1 + \gamma^4 \zeta^2 \left(\frac{C_0}{C_L}\right)^2\right]$$
$$D_3 = 0$$
$$D_4 = Z_F \frac{\alpha_0 \alpha^2}{\gamma^2}$$

(c) *Shear beam*:

$$Z_F = 1 + \frac{2(1+\nu)\gamma^4}{\kappa^2} \left(\frac{C_0}{C_L}\right)^2 \zeta^2$$
$$D_1 = \gamma^4 \zeta^4 (1 + \eta j)$$
$$D_2 = \alpha^2 \left[1 + \frac{2(1+\nu)}{\kappa^2} \gamma^4 \zeta^2 \left(\frac{C_0}{C_L}\right)^2\right]$$
$$D_3 = 0$$
$$D_4 = Z_F \frac{\alpha_0 \alpha^2}{\gamma^2}$$

(d) *Bernoulli-Euler beam*

$$Z_F = 1$$
$$D_1 = \gamma^4 \zeta^4 (1 + \eta j)$$
$$D_2 = \alpha^2$$
$$D_3 = 0$$
$$D_4 = Z_F \frac{\alpha_0 \alpha^2}{\gamma^2}$$

Analysis

The investigation of the problem is covered in two parts:

(a) Effect of the shear effect and rotatory inertia on the total radiated sound power by different beam types.

(b) Effect of the loss factor (η) on the total radiated sound power.

In order to undertake the required investigation equation (13) needs to be numerically evaluated for the case of a steel beam immersed in water. The properties of the beam model analyzed are $E = 20 \times 10^{10}\ N/m^2$, $\rho_v = 7800\ kg/m^3$, $h = 2.54 \times 10^{-2}\ m$, $\nu = 0.3$, $\kappa^2 = 0.85$, $C_0 = 1481\ m/s$ and $\rho_0 = 1000\ kg/m$. The external force strength (f_0) is assumed to be of unit magnitude. By varying the values of parameters M and $K_0 L$, the sound power is computed and then plotted against the wave number ratio (γ) or non-dimensional frequency. The value of η is taken as 0.01 as found in the literature Ungar (1988). However to study the effect of the loss factor, the value of η is varied over 0.9, 0.1, 0.01, 0.001, 0. The effect of η is discussed using a Timoshenko beam. The sound power has been calculated for a variety of combinations of M and $K_0 L$ for the variable beam type and variable loss factor in the frequency range $0.01 < \gamma < 2.2$. The results so obtained are shown. Figures 2 to 4 show the effect of various beam types while Figures 9 and 10 show the effect of various loss factors. For variable beam type, calculations have been done for all the four beams and combined results plotted. For variable loss factor however, these calculations have been undertaken for Timoshenko beam. All calculations have been undertaken using MATLAB.

Discussion

In the Figures shown below, one can see four distinct frequency ranges: the very low frequency region $(\gamma < 0.1)$; the low frequency region $(0.1 < \gamma < 1.0)$; the frequency region near coincidence $(\gamma \sim 1.0)$; and the frequency region above coincidence $(\gamma > 1.0)$ In the low frequency region and in the region above coincidence frequency, the sound powers radiated show no discernible difference. It is the low frequency region and the region near coincidence which is hence of concern to us and needs to be discussed.

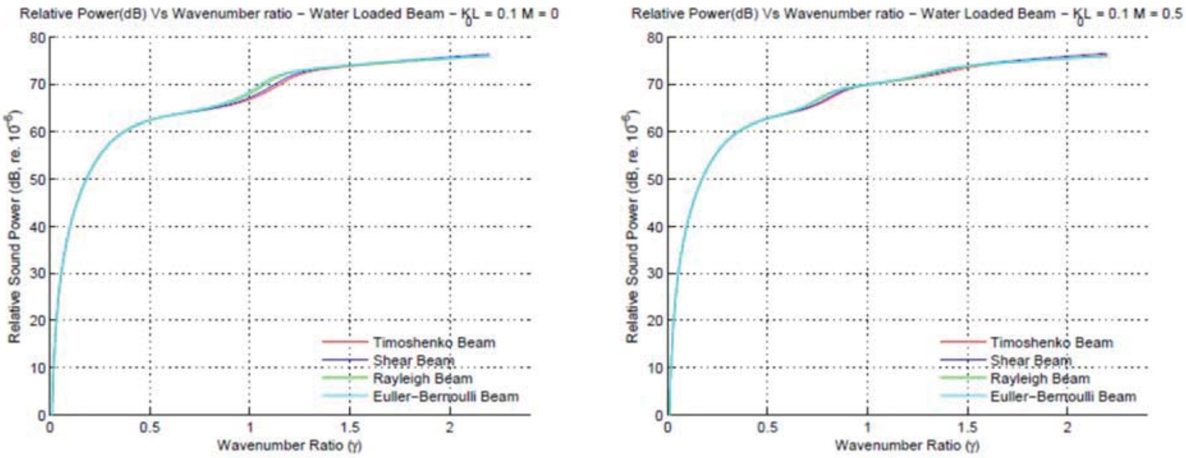

(a) $M = 0$ (b) $M = 0.5$

Figure 2: Relative sound power v/s wave-number ratio for various beam types

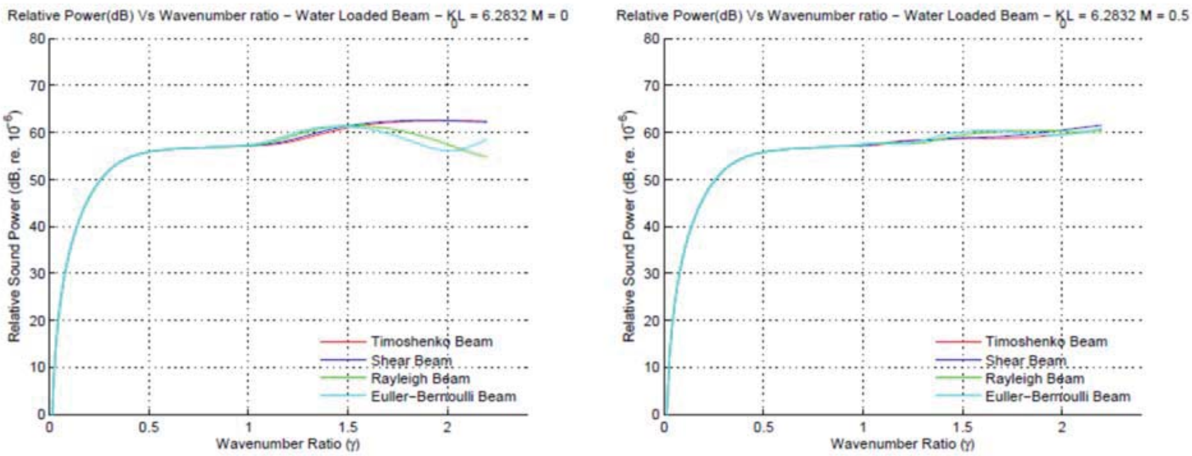

(a) $M = 0$ (b) $M = 0.5$

Figure 3: Relative sound power v/s wave-number ratio for various beam types

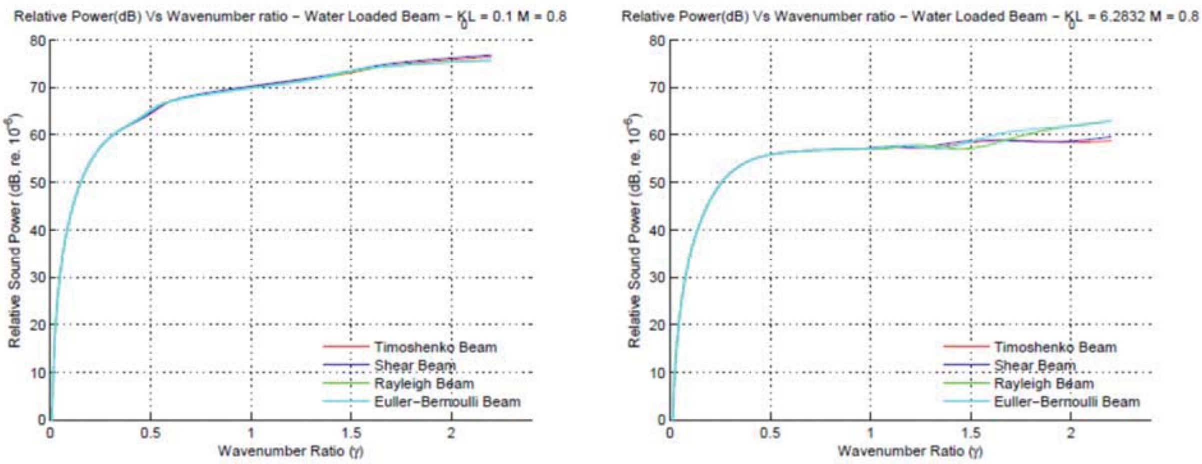

(a) $K_0L = 0.1$ (b) $K_0L = 2\pi$

Figure 4: Relative sound power v/s wave-number ratio for various beam types

Various Beam Type

It is interesting to note that there are no peaks in the sound power curves. The essential lack of peaks for a dense medium like water is due to the proportion of the structural energy converted to acoustic energy. This is larger for dense media, leading to the draining of the radiation energy faster from the structure thus disallowing peak formation. This results in larger effective damping.

Figure 2a and 3a for acoustic length 0.1 and 2π respectively are for Mach number, $M = 0$, which indicates a condition of static load. As expected, the sound radiation from the Timoshenko beam is the least while that of the Bernoulli-Euler beam is a maximum. The effect of Shear beam is greater than Rayleigh beam though within the bounds of Timoshenko Beam and Bernoulli-Euler beam. This effect is as expected view terms of contribution involved in the beams. One notices that for the shear beam, the contributing element is $-\frac{\bar{E}I\rho_v}{\kappa^2\bar{G}}\frac{\partial^4 u(x,t)}{\partial x^2 \partial t^2}$ which is added to the Bernoulli-Euler beam on the LHS and $-\frac{\bar{E}I}{\kappa^2\bar{G}h}\frac{\partial^2}{\partial x^2}$ on the RHS. With the values of κ^2 limited to 0.85 for beams, the contribution of the term shall be greater than 1 thus reducing the net magnitude of the beam impedance Z_m while increasing the acoustic impedance Z_a. This results in a reduced sound output when compared to the sound produced by a Bernoulli-Euler beam. On the other hand for the Rayleigh beam, the contribution is by the term $-\rho_v I \frac{\partial^4 u(x,t)}{\partial x^2 \partial t^2}$ which reduces the structural impedance Z_m. The Rayleigh beam has no effect on the acoustic impedance but since the magnitude of the lowering term on Z_m is large, the net acoustic output is lesser than both the Bernoulli-Euler and the Shear beam. This effect is reversed for frequency regime above coincidence. If we see equation (14), $W \propto \frac{Z_F}{D^2}$, while $D \propto -D_2$. For higher values of γ, for the shear beam, Z_F increases, while D reduces because of increase in D_2. Thus W reduces. Similarly for the Rayleigh beam Z_F remains unchanged while D reduces due to increase of D_2. However $D_{2SE} > D_{2RE}$ and $Z_{FSE} > Z_{FRE}$ thus $W_{SE} < W_{RE}$. $D_{BE} > D_{RE}$ since $D_{2BE} < D_{2RE}$ and $Z_{FBE} = Z_{FRE} = 1$ thus $W_{BE} < W_{RE}$.

With the load moving i.e $M > 0$, and acoustic length being the same, an overall increase in the sound power is observed. Mathematically, as M increases α increases, thus increasing D_2 which leads to reduced D and hence increased W . Physically this is as expected, since with increased speed, the resulting sound is known to increase. However this trend is seen to be reversed for increased frequency the logic being the same as discussed for $M = 0$. It is clear that the increased acoustic length ($K_0 L$) reduces the sound power level over the entire frequency range. This can be attributed to the fact that the total applied force strength is kept constant.

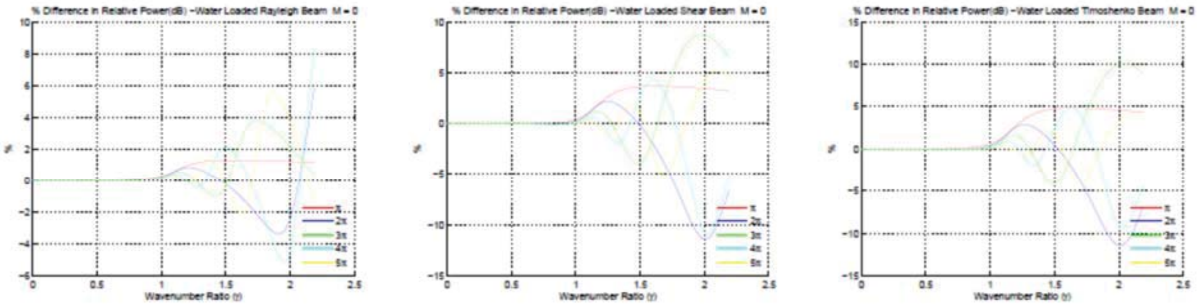

(a) Rayleigh Beam (b) Shear Beam (c) Timoshenko Beam

Figure 5: % Difference in Relative sound power for beams; $K_0 L = n\pi$; $M = 0$

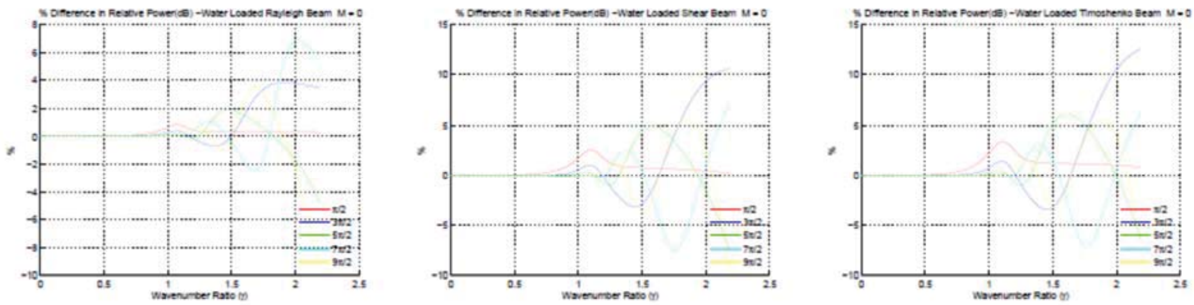

(a) Rayleigh Beam (b) Shear Beam (c) Timoshenko Beam

Figure 6: % Difference in Relative sound power for beams; $K_0 L = (2n-1)\frac{\pi}{2}$; $M = 0$

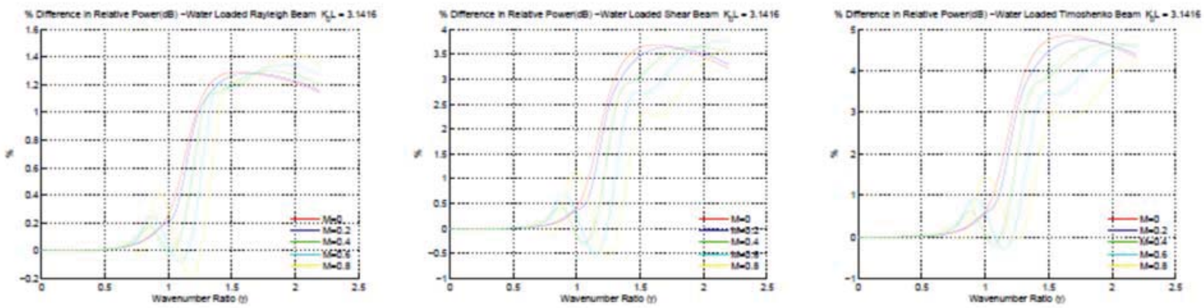

(a) Rayleigh Beam (b) Shear Beam (c) Timoshenko Beam

Figure 7: % Difference in Relative sound power for beams; $K_0 L = n\pi$, various $M

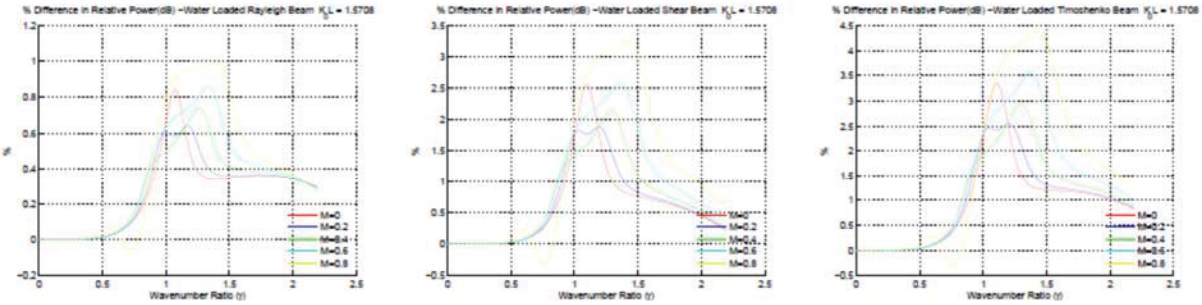

(a) Rayleigh Beam (b) Shear Beam (c) Timoshenko Beam

Figure 8: % Difference in Relative sound power for beams; $K_0L = (2n-1)\dfrac{\pi}{2}$, varying M

In order to analyze the nature of the change in power of various beam types, we reorganize the results as a percentage difference. Since the Bernoulli-Euler beam gives maximum values, we use it as a base value and differences with respect to the values of sound power for Bernoulli-Euler beam are plotted for various beam types. It may be noticed that we have two varying parameters namely M and K_0L. We shall try and understand the contribution of each while varying the other variable. It is interesting to note that if incase K_0L is an integer multiple of π, then the trend of the difference of the total sound power is different than that observed for K_0L being otherwise. The variations are observed for the beam types are shown in Figures 5 and 6 for Rayleigh beam, Shear beam and Timoshenko beam respectively. It is observed that the difference of sound power commences after coincidence if K_0L is an integral multiple of π and at half of coincidence when it is otherwise. The variation of the percentage difference is consistence in trend. For K_0L being an integral multiple of π, $(n-1)$ half modes are visible, where n is the integral multiple of π. However n number of half modes is seen when K_0L is a non integral multiple of π. The reasoning for this is that the beam responds preferentially at $\zeta = K_B$, the free bending wave-number, which is the spatial scale of the propagating or the energy bearing portion of the beam's response at frequency ω. Height of the peak is controlled by the damping present in the structure. Physically, the amount of power radiated is determined by how much energy is available in the force spectrum at the structural / acoustic response wave-number. When this wave number corresponds to an integral multiple of $\dfrac{n\pi}{L}$, there is no energy available in the free spectrum for the conversion to acoustic radiation. These wave-numbers of vanishing energy may be related to wavelength as

$$\zeta = \frac{2\pi}{\lambda} = \frac{n\pi}{L} \Rightarrow \lambda = \frac{2L}{n} .$$

The effect of varying M displays the Doppler shift of the difference curves as the speed increases. The overall pattern that emerges when K_0L is an integral multiple of π and when the value of K_0L is not an integral multiple of π is worth noticing. Special attention may be given to the packing of the values at the critical frequency and the convergence of the data at high wave number ratios.

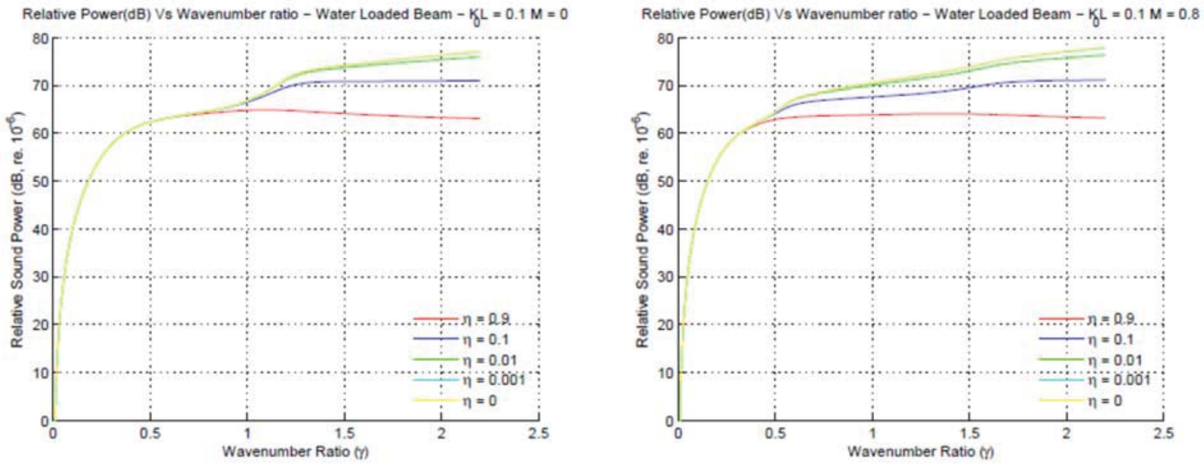

(a) $M = 0$ (b) $M = 0.8$

Figure 9: Relative sound power v/s wave-number ratio for varying η

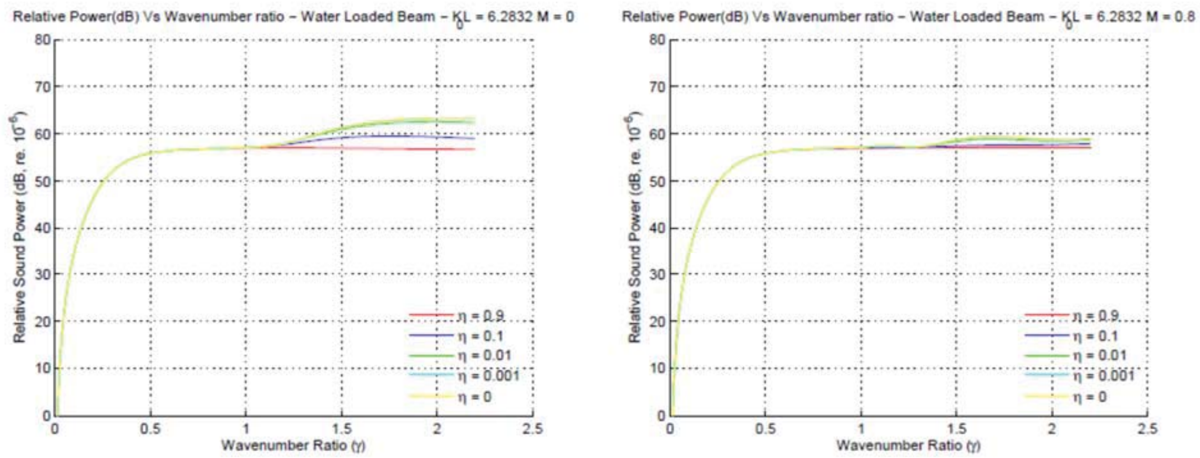

(a) $M = 0$ (b) $M = 0.8$

Figure 10: Relative sound power v/s wave-number ratio for varying η

Loss Factor

Increased vibrational levels due to reduced damping (hence reduced loss factor) lead directly to increased sound radiation as seen in the Figures 9 and 10. It is interesting to note that the curves appear to have the same basic shape. As the structural damping decreases, the amount of steady-state vibrational energy in the beam increases. What is most interesting is that the curves shift up by an amount which is directly proportional to the change in the loss factor. Near the coincidence frequency, if the structural loss is large enough $(\eta \sim 0.1)$, the damping provided by the material exceeds the damping provided by the fluid loading and there is significant difference between the two power curves. If the loss factor is small, then the damping effects reduce and the sound power level significantly increases thus showing that the radiation losses cannot be neglected in this frequency region.

Conclusion

Effect of loss factor, shear effect and rotatory inertia on radiated sound power from beams subjected to moving loads has been investigated. It is concluded that a Timoshenko beam gives the least sound radiation power when compared to the other beam types. The correction for shear effect and rotatory inertia yield results within 4-5 \% more accurate than classical beam theory. The nature of the curves with varying K_0L is dependent on K_0L being an integral multiple of π or otherwise. For varying M , the Doppler shift of the curves is observed for increasing M . The overall pattern that emerges when K_0L is an integral multiple of π and when the value of K_0L is not an integral multiple of π is worth noticing. Special attention may be given to the packing of the values at the critical frequency and the convergence of the data at high wave number ratios. It is observed that as the structural damping decreases, vibrational levels increase thus causing an increase in the sound vibrations. The shift of the curves is however found to be proportional to the change in the loss factor.

Acknowledgement
The first author acknowledges the Indian Navy for the permission to undertake this research work. The authors would like to acknowledge the valuable discussion had with Prof T. Sahoo of Indian Institute of Technology, Kharagpur which has helped in the refinement of the work discussed herein.

References
Cheng C. C. and Chui C. M., (1999). Sound radiation from periodically spring-supported beams under the action of a convected uniform harmonic loading. J. Sound Vib. 226, 83-99

Cheng C. C. Kuo C. P. and Yang J. W., (2000). Wavenumber- Harmonic Analysis of a Periodically Supported Beam under the Action of a Convected Loading, ASME J. Vib. and Acoustics, 122(3), 272-280

Cheng C. C., Kuo C. P. and Yang J. W. , (2001). A Note on the Vibro-Acoustic Response of a Periodically Supported Beam Subjected to a Convected Loading, J. Sound Vib. 239(3), 531-544

Crighton D. G., (1972). Force and moment admittance of plates under arbitrary fluid loading, J. Sound Vib. 20, 209-218

Crighton D. G., (1977). Point admittance of an infinite thin elastic plate under fluid loading, J. Sound Vib. 54, 389-391

Crighton D. G., (1979). The free and forced waves on a fluid loaded elastic plate, J. Sound Vib. 63, 225-235

Crighton D.G., (1983). The Green function of an infinite fluid-loaded membrane, J. Sound Vib. 86, 411-433

Feit D., (1967). Pressure radiated by a point-excited elastic plate, J. Acoust. Soc. Am. 40, 1489-1494

Fryba, L., (1999). Vibration of solids and structures under moving loads. Thomas Telford, London

Gutin L. Y., (1965) Sound radiation from an infinite plate excited by a normal point force, Sov. Phys. Acoust. 10 (4), 369-371

Junger M. C. and Feit D., (1986). Sound Structures and Their Interaction, 2nd Ed., MIT Press, Cambridge, MA

Lord Rayleigh, (1896). The Theory of Sound (2 vols, second edition). London: MacMillan (reprinted 1945 by Dover)

Maidanik G. and Kerwin E . M. Jr., (1967). Influence of fluid loading on the radiation from infinite plates below the critical frequency, J. Acoust. Soc. Am. 40, 1036-1038

Nayak P. R., (1970). Line admittance of infinite is orthotropic fluid-loaded plates, J. Acoust. Soc. Am. 47 (Part 2) 191-201

Morse P. M. and Ingrad K. U. , (1986). Theoretical Acoustics, Princeton University Press, Princeton, New Jersey, 731-732

Keltie R. F. and Peng, H. , (1989). Sound Radiation From Beams Under the Action of Moving Line Forces, ASME J. App. Mech., paper No. 89-APM-19, 1-6

Ungar E. E., (1988). Damping of panels. In Noise and Vibration Control (ed. B. L. E.), chap. 14. Institute of Noise Control Engineering

Willis R. et al., (1851). Preliminary Essay to the Appendix B.: Experiments for Determining the Effects Produced by Causing Weights to Travel over Bars with Different Velocities. In: GREY G. et al.: Report of the Commissioners Appointed to Inquire into the Application of Iron to Railway Structures. W. Clowes and So~s, London 1849. Reprinted in: BARLOW P.: Treatise on the Strength of Timber, Cast Iron and Malleable Iron. London

APPENDIX: LIST OF SYMBOLS

ξ	Wave number variable
$\gamma = \frac{K_0}{K_B}$	Wave number ratio
ν	Poisson's ratio
ρ_v	Mass density of the material
ρ_0	Mass density of the acoustic medium
$\kappa^2 = \frac{\pi^2}{12}$	Cross sectional shape factor or the shear correction factor
η	Loss factor
ζ	Non dimensional wave number variable
$\alpha_0 = \frac{\rho_0 C_L}{\sqrt{12}\ \rho_v C_0}$	Fluid loading parameter
$\delta(x - Vt)$	Delta function
Π	Total acoustic power
h	Height of the beam
$p(x, y = 0, t)$	Acoustic pressure acting on the beam's surface
$u(x,t)$	Transverse displacement of the beam
f_0	Strength of external force per unit width
C_0	Sound speed in the acoustic medium
$C_L = \sqrt{\frac{E}{\rho_v}}$	Longitudinal wave speed
$\bar{E} = E(1 + \eta j)$	Complex elastic modulus
E	Elastic modulus
$\bar{G} = \frac{\bar{E}}{2(1+\nu)}$	Complex shear modulus
$H(x)$	Heavyside step function
$I = \frac{h^3}{12}$	The cross sectional moment of inertia per unit width
$\bar{I}$	Time averaged sound intensity
$M(= \frac{V}{C_0})$	Mach number
$K_0(= \frac{\omega}{C_0})$	Acoustic wave number
$K_B = [\frac{12\rho_v \omega^2}{Eh^2}]^{\frac{1}{4}}$	Free bending wave number
P	Sound pressure on the beam surface
$\dot{U}^*$	Beam surface velocity of conjugation

$\dot{U}\ (= \frac{dU(\xi)}{dt})(= j(\omega + \xi V)U(\xi))$	
V	Subsonic speed of moving force of length 2L
Z_a	Acoustic impedance operator
Z_m	Beam impedance operator
$W = \frac{4\pi\omega(\rho_v h)^2}{\rho_0 f_0^2}\Pi$	Power per unit width

Other quantities and scaled variables are defined as they occur in the text.